Die Bodenkultur: Journal of Land Management, Food and Environment
Volume 70, Issue 3, 171–180, 2019. 10.2478/boku-2019-0015
ISSN: 0006-5471 online, https://content.sciendo.com/view/journals/boku/boku-overview.xml

Research Article

SPECIAL ISSUE
with invited papers from the 47th International Symposium „Actual tasks on Agricultural Engineering“ (ATAE), 5th – 7th March 2019, Opatija, Croatia,
http://atae.agr.hr/, Editor: Prof. Andreas Gronauer

Blooming charge assessment in apple orchards for automatic thinning activities

Beurteilung der Blüte in Apfelplantagen für eine automatische Ausdünnung

Gabriele Daglio*, Raimondo Gallo, Fabrizio Mazzetto

Faculty of Science and Technology, Free University of Bozen (FUB), Piazza Universitá 5, 39100 Bolzano, Italy

* Corresponding author: gabriele.daglio@unibz.it

Received: 2 July 2019, received in revised form: 16 August 2019, accepted: 19 August 2019

Summary

This work aims to develop an automatic system capable of providing objective information about the bloom charge in an apple orchard in order to manage flower-thinning activities. The article presents and discusses the use of a mobile lab (ByeLab) equipped with several optical sensors to carry out a site-specific bloom charge assessment in apple trees. The data collected by the sensors were processed by a specific algorithm implemented in MatLab®. Investigations of the flower reflectance signature indicated that the Normalized Difference Vegetation Index (NDVI) is the most suitable parameter to distinguish leaves from flowers. Pure flowers produce NDVI values slightly negative or at least very near to 0. Despite the homogeneous behavior of the NDVI flower response, OptRx™ sensors, which provide an average assessment of an area, were not able to highlight a significant correlation between the number of flowers and the NDVI values. In the future, further studies will be conducted to assess if other techniques based on image analyses can provide better and more sensitive results regarding the bloom charge assessment. Such results could then be used as a reference in automating machines for thinning operations according to a site-specific approach.

Keywords: optical sensors, mobile lab, precision farming, ground based sensing, vegetation index

Zusammenfassung

Ziel dieser Arbeit war es, ein System zu entwickeln, das automatisch objektive Informationen über die Blütendichte in Apfelplantagen liefert und als Instrument für die Ausdünnung von Blüten verwendet werden kann. Üblicherweise wird dieser Vorgang, basierend auf der persönlichen Erfahrung des Arbeiters, manuell durchgeführt. In diesem Beitrag wird die Verwendung eines mobilen Labors (ByeLab) zur ortsspezifischen Beurteilung der Blütendichte von Apfelbäumen mithilfe optischer Sensoren vorgestellt und diskutiert. Das Byelab wurde mit mehreren Sensoren ausgestattet, darunter einem GNSS-RTK-System, drei optischen Sensoren (OptRx™), zwei LiDAR-Sensoren und einer Inertialen Messeinheit (IMU). Während OptRx™ und LiDAR verwendet wurden, um den Vegetationsindex (VI) bereitzustellen und das Oberflächenprofil des gescannten Baldachins zu erfassen, wurden mit der GNSS-RTK-Einheit alle vom optischen Sensor und den LIDARs erfassten Daten georeferenziert. Schließlich wurde die IMU verwendet, um das Rauschen und Verzerrungen der erfassten Daten aufgrund der durch die Bodenunebenheiten erzeugten Vibrationen zu korrigieren. Eine LabView-Anwendung wurde verwendet, um die von den Sensoren erfassten Daten zu synchronisieren. Anschließend wurden alle Messungen von einem in MatLab® implementierten Algorithmus verarbeitet. Im April 2018 wurden drei Erhebungen durchgeführt, um die gesamte Blütezeit abzudecken: Blühbeginn, Vollblüte und Ende der Blüte. Untersuchungen zur Blütenreflexionssignatur haben ergeben, dass der Normierte Differenzierte Vegetationsindex (NDVI) der am besten geeignete Parameter zur Unterscheidung zwischen Blättern und Blüten ist. In der Tat hat der NDVI-Wert eine negative Korrelation mit der Blütendichte, da reine Blüten leicht negative NDVI-Werte aufweisen, jedenfalls sind sie sehr nahe bei 0. Trotz der gleichmäßigen NDVI-Messungen der Blüten konnte die Verwendung von OptRx™-Sensoren keine signifikanten Korrelationen zwischen der Anzahl der Blumen und den NDVI-Werten aufzeigen, da sie eine durchschnittliche Bewertung einer Fläche zurückgeben. In Zukunft werden weitere Studien durchgeführt, um zu beurteilen, ob andere auf Bildanalysen basierende Techniken bessere und empfindlichere Ergebnisse in Bezug auf die Bewertung der Blütendichte liefern können. Diese Ergebnisse könnten als Referenz für die Automatisierung von Maschinen verwendet werden, die bei Ausdünnungsvorgängen nach einem standortspezifischen Ansatz eingesetzt werden.

Schlagworte: Optische Sensoren, mobiles Labor, Präzisionslandwirtschaft, bodenbasierte Sensorik, Vegetationsindex

1. Introduction

Flower thinning is one of the most important agronomical operations conducted in apple orchard management. Generally, a portion of the flowers must be removed early in the growing season to ensure that the flowers and the subsequent fruits are present in appropriate amounts. The quantity to be thinned depends on the bloom intensity. This procedure can be performed with manual or with mechanical methods or through the spraying of chemicals products (Xiao et al., 2014; Dias et al., 2018). The two last methods are used to reduce costs. Manual thinning requires more money and time but may be necessary if chemical thinning proves to be inadequate because of its inability to consider the variability between individual trees (Aggelopoulou et al., 2010). In order to perform a thinning operation correctly, it is necessary to estimate the density of the blooming charge. Usually, this procedure is carried out by specialized operators trained in the procedure. In order to reduce the time required for this assessment, ground and remote-sensing technologies can be used to automate it. Indeed, with the use of optical sensors installed on vehicles (aerial or terrestrial), it is possible to obtain punctual information about a crop, such as bloom charge, canopy volume, distance between plants, number of plants, or health status (Rosell et al., 2009; Di Gennaro et al., 2016; Albetis et al., 2017; Gallo et al., 2017; Ristorto et al., 2017). In order to find new solutions for automating crop-monitoring activities, several types of sensors (including LiDAR and OptRx™) have been tested by several authors. The LiDAR (Light Detection and Ranging) sensor is able to assess the canopy volume via the emission of a laser beam (Bietresato et al., 2016; Vidoni et al., 2017), while active light sensors are able to provides information about the status of the crop (Mazzetto et al., 2010; D'Auria et al., 2016). Active optical sensors, such as OptRx™, are able to generate a light at three known wavelengths (670, 730, and 780 nm) and record the light reflected by the target. Given the value of the recorded reflectance, the OptRx™ can compute two vegetation indices (VIs): the Normalized Difference Vegetation Index (NDVI) and the Normalized Difference Red Edge Index (NDRE). Recent studies reveal the application of optical devices in apple orchards for different purposes. A Charge-Coupled Device (CCD camera) was tested and used by Gongal et al. (2018) to develop a machine vision system to estimate the apple fruit size in the tree canopy. Dias et al. (2018) and Hočevar et al. (2013) used multiple cameras and an industrial color camera with the aim of detecting apple flowers through a deep convolution network and to estimate the apple flower charge by image analysis. This article describes a mobile laboratory equipped with several sensors, called the ByeLab (Bionic Eye Laboratory), and an evaluation of its capability of providing objective information about the bloom charge in apple orchards with the aim of determining if it could be used to manage flower-thinning activities.

2. Materials and methods

2.1 In-field surveys

The main equipment used for the crop-monitoring activities in this study is the ByeLab. This prototype mobile laboratory (Figure 1) is a tracked bin-carrier (NEO Alpin by Windegger S.r.l., Lana, Bolzano, Italy) which has been modified with a metal structure and had several sensors installed. The vehicle is powered electrically, controlled via wireless remote control, and has compact dimensions. These features ensure its inter-row, high-agility performance as well as its transmission of low vibrations. For this experiment, the mobile laboratory was equipped with the following:

- a GNSS-RTK system (GEOMAX Zenith 35) with 20 Hz of sampling, placed on the top of the vehicle;
- three OptRx™ AgLeader optical sensors with 10 Hz of sampling, placed 0.8, 1.6, and 2.4 m from the ground;
- two LiDARs (SICK LMS111) with 50 Hz of sampling, placed at 0.95 and 2.5 m from the ground;
- an inertial measurement unit (IMU) (LMRK 10 AHRS) with 10 Hz of sampling;
- a control unit system.

OptRx™ and LiDAR sensors were installed in order to ensure proper canopy coverage at a 3.5-m height, the common height for apple training systems in productive orchards in South Tyrol. OptRx™ sensors were used because, as already demonstrated in other crop-monitoring applications, they are of high utility in precision agriculture applications because of their cheapness, robustness, and quick real-time responses (Maharlooei et al., 2014). These optical sensors were used to collect data related to the reflectance of the monitored canopy, while LiDARs were used to investigate canopy thickness. The roll, pitch, and yaw angles acquired by an inertial measurement unit (IMU) were used to correct the ByeLab's trajectory and

Figure 1. The figure shows the ByeLab used during the survey, the sensors mounted on the metal structure (on the left of the three OptRx™ sensors, on the central pole: (i) the GNSS receiver, (ii) the two LiDARs, and (iii) the IMU) and on the white structure the computer
Abbildung 1. Die Abbildung zeigt das bei der Vermessung verwendete ByeLab, die an der Metallstruktur montierten Sensoren (links die drei OptRx ™ -Sensoren, am Mittelpol: i) den GNSS-Empfänger, ii) die beiden LiDARs und iii) die IMU) und auf der weißen Struktur den Computer

to adjust all the acquisitions. Indeed, the terrain roughness (because of the presence of grass, stones, and holes) affected the vehicle tracking, causing slight noises in the collected data. All the collected data were georeferenced by an GNSS-RTK system.

As the installed sensors had different acquisition frequencies, all the collected data were first synchronized by a procedure implemented in the LabView® code running on the control unit. Then the recorded data were post-processed by dedicated interpretative algorithms developed in MatLab® environment, as explained in the next section.

The testing area consisted of one orchard row of plants of the *Malus domestica* variety Kanzi® located at the "Azienda Sperimentale Laimburg," Bolzano, Italy. The row was divided into several transect according to the training system used (2D and Spindel) (Figure 2). At the beginning of the flowering season, a manual count of the flowers was made to ascertain the real number of flowers in every meter of the row. These data were then compared with those collected by the ByeLab in order to carry out a validation of the acquisition system. Three surveys with the ByeLab were carried out in April 2018 in order to detect the blooming charge during the whole blooming period. These surveys were performed in the pre-, full-, and post-blooming periods (Figure 3). To obtain reliable data related to the flower and leaf reflectance, three surveys were performed and then averaged.

In order to better evaluate the features of the flower reflectance signatures, some preliminary investigations were performed before running the ByeLab field tests. To this aim, a portable spectrophotometer (Jaz Ocean Optics Spectrometers) was used. The information collected by this tool was then used to better understand the reflectance behavior of different plant organs (petals, corolla, flowers, leaves, trunks). Considering the acquisitions on red, near infrared (NIR), and RedEdge wavelengths, because the same information would be acquired by the OptRx™, three VIs were tested: NDVI, NDRE, and White Flower Index (WFI). The WFI is an index able to discriminate the white components, i.e. flowers, from the green ones (vegetation). It is calculated through the following equation:

$$WFI = \frac{|Red\text{-}NIR|}{|Red\text{-}RedEdge|}$$

Figure 2. The two training systems in the row used: 2D system (left) and Spindel (right)
Abbildung 2. Die beiden Trainingssysteme in der betrachteten Reihe: 2D (links) und Spindel (rechts)

Figure 3. From left to right: apple tree in the pre-, full-, and post-blooming stages
Abbildung 3. Von links nach rechts: Apfelbäume in den drei Entwicklungsstadien Blühbeginn, Vollblüte und Ende der Blüte

The data obtained by the OptRx™ assessment were compared and validated with the manual flower count.
The information related to the canopy thickness collected by the LiDARs mounted on the ByeLab was validated using a terrestrial laser scanner (TLS) (model CAM2 FARO). The raw data collected by TLS were elaborated upon with FARO Scene 7.1.1 software in order to obtain a 3D model to compare with the data obtained by LiDARs.

2.2 The algorithm for data interpretation

Thanks to the LabView synchronization, all data collected by the different sensors were stored automatically in a unique record instead of a single file data set. Each acquired file, using a post-processing procedure implemented in MatLab® environment, was interpreted and translated into information. Generally, data acquisitions were performed separately for each semi-row investigated (up to step number 4 below) and merged together during the elaboration procedures to compose the entire row. The procedure followed is described in more detail below:

1. Removal of partially completed records: The analysis starts with the loading and verification of the data stored in the temporary memory of the on-board control unit. The algorithm code expects that each record will be structured in eight strings. Should some data be lacking, the script deletes the entire record and proceeds with the next step, during which specific functions and parameters complete the reading of the files and the checking of the expected size of the measurements of each sensor. At this stage, the file data sets are structured in columns containing:
   - a one-time string, where progressive acquisition time has been reported;
   - two LiDAR strings, where measurements of angles and distances from both LiDARs have been reported (high and low);
   - one IMU string, where angle of pitch, roll, and yaw have been reported;
   - three VI strings, where the reflectance values collected for the red, NIR, and RedEdge wavelengths have been reported; and
   - one GNSS string, where data related to vehicle's coordinates and speed have been reported.

   If the data process procedure finds records without the expected number of strings, the entire record is removed. The use of incomplete records causes the failure of the data processing.

2. Point cloud analysis and noises filtering: The second step of the algorithm procedure foresees the displacement of each point collected by the two LiDARs into the space. As it knows the distances between the LiDARs and targets as well as the scanning angle, the system is able to build a point cloud related to the scanned semi-row. The obtained data set is corrected using the information on roll, pitch, and yaw collected by the IMU. Thanks to this procedure, all the noises caused by terrain unevenness, such as changes in the routing or displacements of the metal frame where the

sensors are installed, are corrected. In order to reduce the risk of estimation errors, the algorithm carries out a noise-filtering procedure. As a result, the collected point cloud is cut at a height lower than 0.3 m and higher than 3.8 m. Consequently, for the following procedures, the algorithm considers only the effective canopy wall without taking into consideration the eventual herbaceous layer or outliers above the canopy. The goal of this filtering is the removal of data that may generate disturbances in the analytical procedures and, at the same time, to reduce the computation time required by the process.

3. Roto-translation of the point cloud to a local system of reference and the merging of the two semi-canopies: After the point cloud noise correction, the semi-row data sets are then plotted into the space according to the coordinates collected by the RTK-GNSS unit. To perform the union between the left side and right side of the canopy, a roto-translation of the point cloud is necessary; therefore, the data set is plotted in a local reference system. Consequently, both semi-canopies are displaced following the same direction. To define a proper intersection plane between the two canopy sides, it is necessary to define, through a manual selection of common points present on both point clouds, a potential center line of the apple row. For this process, the poles along the row are used as references. Thanks to this operation, the origin of the reconstructed canopy is arbitrarily set-up in the bottom left corner of the center line plane in order that the x-, y-, and z-axes correspond to the depth, length, and height of the row, respectively. In the end, the algorithm calculates the distance of each point to the center line in order to obtain the canopy thickness (Figure 4).

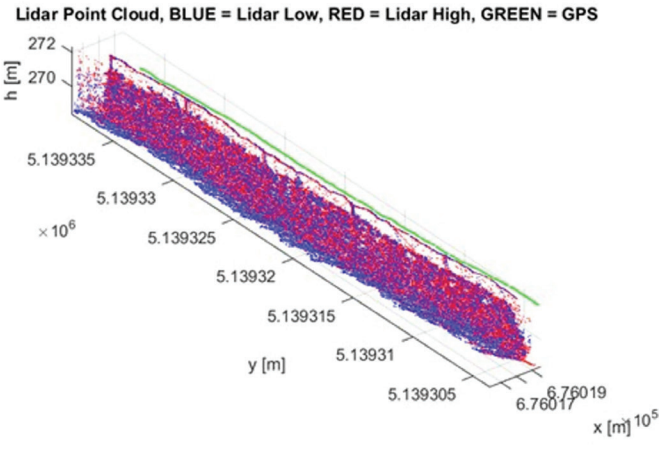

Figure 4. Example of an output of the LiDAR data elaboration
Abbildung 4. Beispiel für die Ausgabe von LiDAR-Daten

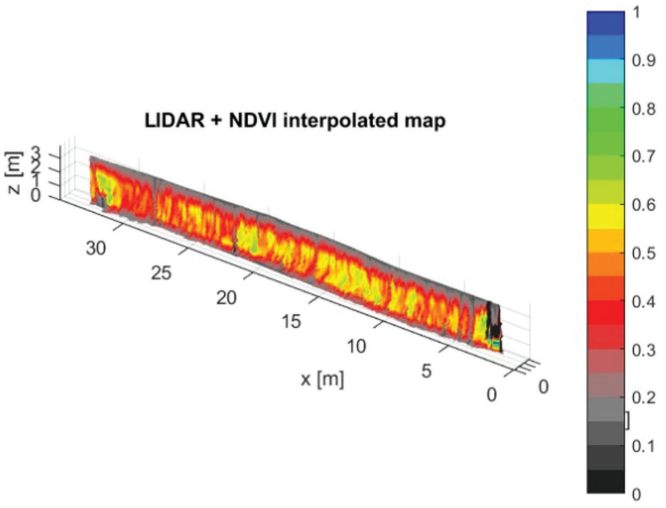

Figure 5. Output from merging the LiDAR and OptRx™ data
Abbildung 5. Ausgabe und Zusammenführung von LiDAR- und OptRx™ -Daten

4. Overlay of the OptRx™ acquisitions: When the point cloud is placed in the local system of reference, the algorithm overlays the information collected by the OptRx™ sensors. Thanks to the data synchronization performed during the acquisition and through the parameters used for the previous roto-translation, the analytical procedure is able to carry out a precise overlapping of both detections. At the end of this procedure, the merging of the points collected by the LiDAR and OptRx™ sensors is obtained (Figure 5).
5. Canopy segmentation for data assessment: By using the y- and z-planes of the combined data set, a reference grid is overlapped temporarily on the cloud point. The bottom left corner of the grid is placed at coordinate (0, 0.4) of the local reference system. The offset in the positioning of the grid is performed in order to have the barycenter of each cell at the same height as the OptRx™ sensors. Therefore, the grid is composed of three rows of cells of 1 m in length and 0.8 m in height, and the total number of cells depends on the length of the monitored row. The application of this grid permits the identification of several samples of the synchronized data set with which carry out the thickness and VI analysis.

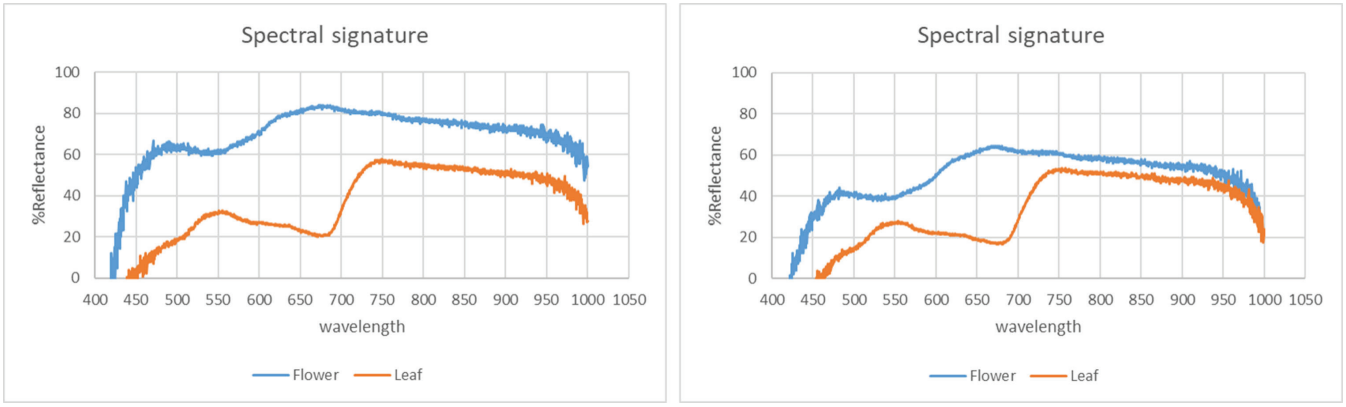

Figure 6. Spectral signatures of two sets of flower and apple leaves collected from different trees
Abbildung 6. Spektrale Signatur von zwei Paaren von Blüten- und Apfelblättern, die von verschiedenen Bäumen gesammelt wurden

6. Thickness and bloom charge assessment: The last step of the data analysis concerns the assessment of the canopy thickness and the evaluation of the blooming charge. To obtain this information, the average value of the distances related to the portion of the point cloud and VI inside each cell of the overlapped grid are computed. As a final output, a summary table, together with a thematic map, is obtained for each monitored row. Both outputs consider the left and right sides of the row from its origin, while the table reports the numerical values of detection results for each cell, and the maps describe the same information using a qualitative approach. Indeed, thanks to a predefined set of colors and histogram lengths, the information related to canopy thickness and VI can be shown. The colors represent the classification of the VI values (white and yellow represent high and moderate blooming charges, respectively, while cyan and green represent moderate and high amounts of leaves, respectively), while the histogram heights represent the canopy thickness along the monitored row.

3. Results and discussion

From the analysis of the spectral signature (Figure 6), it is possible to see that for the same plant organs (flowers and leaves) collected from different trees, the spectrums always have similar patterns but different values when the same wavelength is considered. This result probably occurs because during the in-field survey, the acquisition, even if performed under the same operative conditions and using the same procedure, may be affected by human errors during data acquisition. Indeed, slight movements of the probe over the sample or different distances between the probe and target affected the final acquisition of the spectrum.

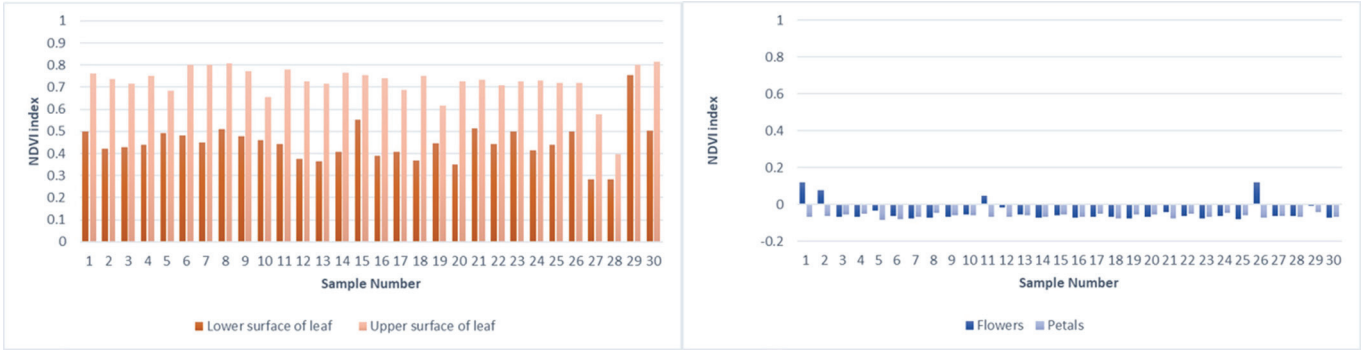

Figure 7. NDVI index associated with lower and upper surfaces of leaves (left) and flowers and petals (right). Pure flowers show NDVI values that are slightly negative or at least very near to 0
Abbildung 7. NDVI für die untere und obere Blattfläche (links) sowie für Blüten und Blütenblätter (rechts). Reine Blüten zeigen leicht negative NDVI-Werte, jedenfalls sehr nahe bei 0

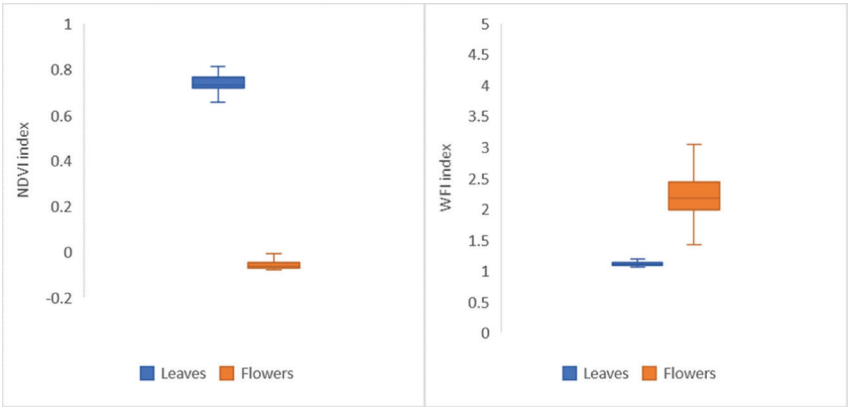

Figure 8. Box and whisker plots of the NDVI and WFI associated with leaves (in blue) and flowers (in orange). The boxes show the values of the VIs obtained via the reflectance values measured with the portable spectrophotometer on 30 leaves and flowers of apple trees
Abbildung 8 Box- und Whisker-Plots von NDVI- und WFI-Index für Blätter (blau) und Blüten (orange). Die Boxen zeigen die Werte der VIs, die durch die Reflexionswerte erhalten wurden, welche mit dem tragbaren Spektralphotometer an 30 Blättern und Blüten bei Apfelbäumen gemessen wurden

By calculating the three VIs using the reflectance records collected by the OptRx™, it has been possible to determine that the NDVI is the most suitable parameter to use to discriminate leaves from flowers. Moreover, it was observed that low and high NDVI values correspond to the flowers and leaves, respectively (Figures 7 and 8).

Considering the values of the NDVI associated to the flowers and leaves and the elaboration of the data collected via the ByeLab, we expect a negative correlation between the NDVI value and number of flowers: the lower the NDVI value, the higher the blooming charge. In Figure 9, the potential behavior between the number of flowers and NDVI value is reported. The obtained results (Figure 10) showed very poor correlation between NDVI values and number of flowers, where the expected negative correlation is not highlighted. This is probably due to the fact that the manual counting of the flowers gives too detailed information about the blooming charge, while the OptRx™ sensor returns averaged values of the VI of the monitored surface. Moreover, the value of NDVI could be influenced by background noise. Nevertheless, considering the different blooming periods, the NDVI showed difference between the full blooming period and the others (pre- and post-blooming). Comparing the TLS and ByeLab (LiDAR) scans, there is a slight stretching of the point cloud collected by the ByeLab. Consequently, all the measurements collected by the system are not precise (Figure 11), perhaps because of a time delay in the communications with LiDAR and the Global Position System (GPS) as a result of a difference in acquisition frequencies. In addition, it is possible that the characteristics of the two survey systems themselves could cause the abovementioned inaccuracy: the TLS carries out static measurements, while the ByeLab does dynamic assessments. However, from the point cloud collected by the proposed mobile laboratory, it is possible to obtain, even if approximately, important information, such as the change in training, the thickness of the canopy, the identification of small plants, gaps between plants, and the poles of the irrigation and training systems. All this information can be used to recreate a virtual 3D orchard.

Figure 9. Potential correlation between the NDVI value and number of flowers
Abbildung 9. Potenzielle Korrelation zwischen NDVI-Werten und der Blütenmenge

Another output of the analytical procedure is the qualitative descriptive map (Figure 12), which is related to the coverage of the flowers and the thickness of the canopy at three different heights. This remarkable qualitative result was obtained by merging the LiDAR and OptRx™ data. White and yellow

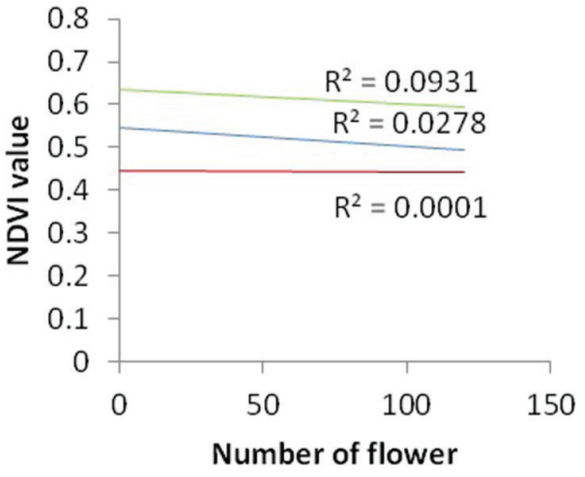

Figure 10. Trend of NDVI values for the canopy during the monitoring period. The blue line represents the correlation between NDVI value and number of flowers in pre-blooming, the red one in full blooming, and the green one in post-blooming.
Abbildung 10. Trend der NDVI-Werte für den Baldachin während des Überwachungszeitraums. Die blaue Linie stellt die Korrelation zwischen dem NDVI-Wert und der Anzahl der Blüten in der Vorblüte dar, die rote in voller Blüte und die grüne in der Nachblüte.

colors have been associated with low NDVI values, that is, a high number of flowers, whereas cyan and green colors have been associated with high NDVI values, that is, a low-blooming charge. The system's output highlights that in the pre-blooming period, that is, the absence of flowers, the predominant color of the map is cyan and not green. This result could be due to the fact that the leaves are still small and cannot be perceived clearly by the sensors. In full bloom, the predominant colors are white and yellow because the flowers are out and cover a large portion of the green vegetative surface of the plants. Meanwhile, in the post-blooming period, the cyan and green classification are the predominant because the presence of the flowers is very low, and, on the contrary, the leaf volume is very large. Therefore, during this acquisition, the sensors acquire reflectance values that permit the system to calculate NDVI values around 0.7, which represent healthy and green apple vegetation.

The results obtained from this analysis are not comparable with those present in the literature. Several authors (Hočevar et al. 2013; Xiao et al., 2014; Dias et al., 2018) have estimated the blooming charge of apple tree plants using methods based on image analysis. In their research, the images were usually acquired with mono and/or multi spectral cameras mounted on unmanned aerial vehicle (UAV) systems, tractors, or static supports. The use of these sensors determines overestimations of the bloom charge assessment because of trees overlapping, high reflection on leaves, background noise, and the low resolution of the used camera. The system described here gives back information about the blooming charge assessment using cheap active sensor already available on the market, which returns NDVI values suitable to be used directly on the computation procedures. Thanks to the use of the OptRx™, sensors issues related to surrounded light conditions have been overcome. Besides this, thanks to the RTK-GNSS installed on the ByeLab, the developed system is able to georeference all the acquisition and gives high detailed information on the placement of the blooms.

4. Conclusions

Despite the homogeneous behavior of the NDVI flower response, the OptRx™ sensors were not able to highlight a significant correlation between the number of flowers and the NDVI values. Thus, mono-dimensional sensors—such

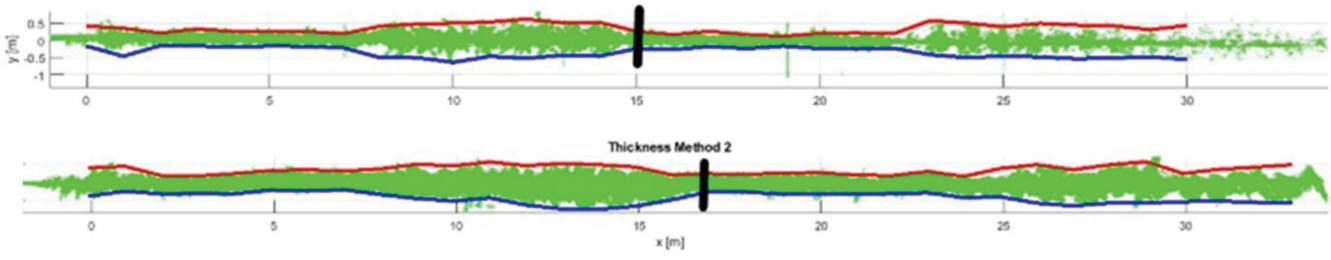

Figure 11. Top-view TLS (above) and ByeLab (below) scans of the row. The point of change in the training system is indicated in black. It is visible in the stretching between the two scans.
Abbildung 11. TLS-Scan (oben) und ByeLab-Scan (unten) einer Reihe. Der Punkt des Wechsels im Trainingssystem ist in Schwarz angezeigt. Die Dehnung zwischen den beiden Scans ist erkennbar.

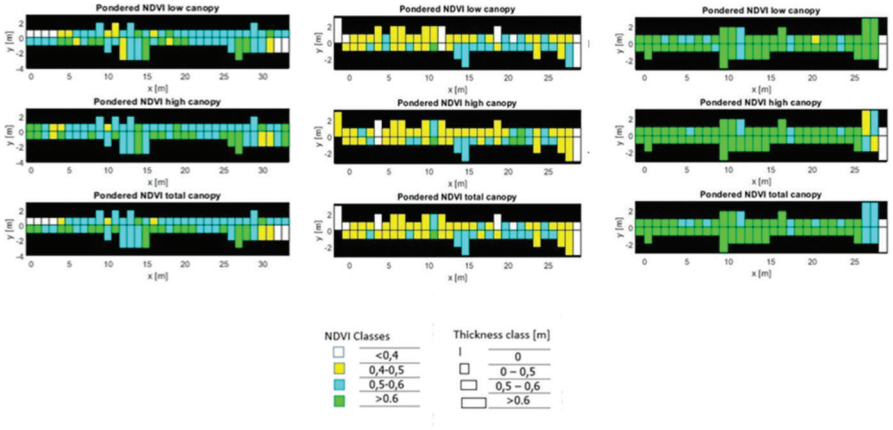

Figure 12. Descriptive maps of a row divided into equal sections along the longitudinal axis showing NDVI classes (white and yellow represent high and moderate blooming charges, respectively, while cyan and green represent moderate and high amounts of leaves, respectively) and thickness classes for the canopy during the blooming period.
Abbildung 12. Beschreibende Karten einer Reihe, die in gleiche Abschnitte entlang der Längsachse unterteilt sind, und die NDVI-Klassen (Weiß und Gelb stehen für eine hohe bzw. moderate Blütendichte; Cyan und Grün stehen für eine moderate und hohe Anzahl von Blättern) und Dickenklassen des Blätterdaches während der Blütezeit.

as the OptRx™—do not seem suitable for the estimation of the flower charge. To increase the reliability of the system, a higher number of sensors per side (4 or more instead of 3) will be investigated in future field tests. However, the combination of LiDAR and OptRx™ data has improved the quality of detection. In fact, by merging the data collected by the two types of sensors, it is possible to build descriptive maps providing information on canopy thickness and VI values, which can be used as references for automated machines conducting thinning or pruning operations according to a site-specific approach.

In order to propose future applications of a system that is able to provide information about the condition of the crop in real time, it is necessary to evaluate the amount of time required for computation, that is, if it is possible to use such a system in practice. It would be useful to evaluate the use of different algorithms and to study the correlations obtained by setting filters that give greater importance to the lower NDVI values found in the investigated areas. To overcome the problem of the mono-dimensional scans obtained through the OptRx™ sensors, bidimensional scans with pixel matrix generation, such as those provided by a multi-camera set-up, should be considered and tested together with the LiDARs. In this case, we expect the system to be capable of coloring each point of the acquired point cloud with the information collected by the cameras. Therefore, thanks to this approach, it should be possible to pinpoint the origin of each point of the cloud and consider only needs to be assessed.

References

Aggelopoulou, K.D., Wulfsohn, D., Fountas, S., Gemtos, T.A., Nanos, G.D. and S. Blackmore (2010): Spatial variation in yield and quality in a small apple orchard. Precision Agriculture 11, 538–556.

Albetis, J., Duthoit, S., Guttler F., Jacquin, A., Goulard, M., Poilvé, P., Féret, J.B. and G. Dedieu (2017): Detection of Flavescence dorée Grapevine Disease Using Unmanned Aerial Vehicle (UAV) Multispectral Imagery. Remote Sensing 9, 308.

Bietresato, M., Carabin, G., Vidoni, R., Gasparetto, A. and F. Mazzetto (2016): Evaluation of a LiDAR-based 3D-stereoscopic vision system for crop-monitoring applications. Computers and Electronics Agriculture 124, 1–13.

D'Auria, D., Ristorto, G., Persia, F., Vidoni, R. and F. Mazzetto (2016): Development and preliminary tests of a crop monitoring mobile lab based on a combined use of optical sensors. International Journal of Computer & Software Engineering 1, 103.

Dias, P.A., Tabb, A. and H. Medeiros (2018): Apple flower detection using deep convolutional networks. Computers in Industry 99, 17–28.

Di Gennaro, S.F., Battiston, E., Di Marco, S., Facini, O., Matese, A., Nocentini, M., Palliotti, A. and L. Mugnai (2016): Unmanned Aerial Vehicle (UAV)-based remote sensing to monitor grapevine leaf stripe disease within

a vineyard affected by esca complex. Phytopathologia Mediterranea 55, 262–275.

Gallo, R., Ristorto, G., Daglio, G., Massa, N., Berta, G., Lazzari, M. and F. Mazzetto (2017): New solutions for the automatic early detection of diseases in vineyards through ground sensing approaches integrating lidar and optical sensors, Chemical Engineering Transactions 58, 673–678.

Gongal, A., Karkee, M. and S. Amatya (2018): Apple fruit size estimation using a 3D machine vision system. Information Processing Agriculture 5, 498–503.

Hočevar, M., Širok, B., Godeša, T. and M. Stopar (2014): Flowering estimation in apple orchards by image analysis. Precision Agriculture 15, 466–478.

Maharlooei, M., Sivarajan, S., Nowatzki, J., Bajwa, S.G. and H. Kandel (2014): Evaluation of in-field sensors to monitor nitrogen status in soybean crops. 12th International Conference on Precision Agriculture, 20–23 July 2014, Sacramento, California, International Society of Precision Agriculture.

Ristorto, G., Gallo, R., Gasparetto, A., Scalera, L., Vidoni, R. and F. Mazzetto (2017): A mobile laboratory for orchard health status monitoring in precision farming. Chemical Engineering Transactions 58, 661–666.

Rosell, J.R, Llorens, j., Sanz, R., Arnó, J., Ribes-Dasi, M., Masip, J., Escolá, A., Camp, F., Solanelles, F., Gràcia, F., Gil, E., Val, L., Planas, S. and J. Palacin (2009): Obtaining the three-dimensional structure of tree orchards from remote 2D terrestrial LIDAR scanning. Agricultural and Forest Meteorology 149, 1505–1515.

Xiao, C., Zheng, L., Sun, H., Zhang, Y. and M. Li (2014): Estimation of the apple flowers based on aerial multispectral image. American Society of Agricultural and Biological Engineers, Paper No. 141912593.